Applied Mathematical Modelling 36 (2012) 1731–1751

Contents lists available at SciVerse ScienceDirect

Applied Mathematical Modelling

journal homepage: www.elsevier.com/locate/apm

A complete analysis of axial piston pump leakage and output flow ripples

J.M. Bergada [a,*], S. Kumar [a], D.Ll. Davies [b,1], J. Watton [b,1]

[a] Fluid Mechanics Department, ETSEIAT-UPC, Colon 11, Terrassa 08222, Spain
[b] Cardiff School of Engineering, Cardiff University, Queen's Buildings, The Parade, Cardiff CF24 3AA, Wales, UK

ARTICLE INFO

Article history:
Received 23 June 2010
Received in revised form 29 August 2011
Accepted 1 September 2011
Available online 12 September 2011

Keywords:
Leakage on piston pumps
Piston pump pressure/flow dynamics
Piston pump dynamic model

ABSTRACT

The paper is focused on understanding the flow losses and the resulting flow/pressure dynamics in a piston pump. Initially, equations to evaluate leakages in all piston pump gaps will be presented and tested against numerical models, later the equations will be linked to determine the general pressure/flow pump dynamic characteristics. The model will also provide the temporal pressure in each piston/cylinder chamber and the temporal leakage in all pump clearances. A test rig able to measure the dynamic pressure inside a piston chamber was build and employed to evaluate pressure ripple dynamics as a function of turning speed, outlet pressure and swash plate angle. The comparison between experimental and simulated results is very good, giving confidence to the model presented. The advantage of using the analytical approach is that explicit equations allow a more direct understanding of the effect of dimension changes and operating conditions on pump dynamics. Fluid used hydraulic oil ISO 32.

1. Introduction

In theory the study of the piston-cylinder pressure ripple should be straightforward, since the differential equation involved is well known. The cylinder temporal pressure differential equation, depends on the leakage across the different piston pump clearances, but the dynamic equations linking the leakage across each piston pump gap and the pressure differential across the gap are not fully known. To overcome this difficulty several researchers have used different approaches, Foster and Hannan [1], integrate the dynamic pressure differential equation of the cylinder and evaluate the leakage experimentally, an interesting point in this paper is that they take into account the effect of the oil volume at the inlet and delivery lines, the paper introduces a link between pressure transients into the cylinder and the noise generated by the pump. Manring [2–4] assumes all leakage flows as laminar and uses a linear relation between pressure drop and flow, being necessary to find the leakage constant for every pump clearance. Ivantysynova et al. [5–9] integrate the Reynolds equation of lubrication, linked with the energy equation to evaluate dynamically every leakage, pressure distribution and temperature in all piston pump clearances. The implicit solution is performed via a numerical computer program, with all computer sub-routines linked to create a macro program called CASPAR which evaluates the entire pump behaviour.

Very recently Ma et al. [10] presented a single and multi-cylinder piston pump dynamics, in where they considered some typical equations to evaluate the leakage across the different piston/barrel gaps. They studied very carefully the leakage across the triangular timing grooves; they also considered the fluid inertia of the timing grooves, the simulated pressure

* Corresponding author.
E-mail addresses: bergada@mf.upc.edu (J.M. Bergada), kumarsush@gmail.com (S. Kumar), daviesdll@cardiff.ac.uk (D.Ll. Davies), wattonj@cardiff.ac.uk (J. Watton).
[1] Tel.: +44 2920876830.

0307-904X/$ - see front matter © 2011 Elsevier Inc. All rights reserved.
doi:10.1016/j.apm.2011.09.016

Nomenclature

A,C,E,G,I,K,M,O,Q,S,U	piston constants (m^2/s)
B,D,F,H,J,L,N,P,R,T,V	piston constants (N/m^2)
A_c	piston chamber outlet area (m^2)
A_{valve}	valve outlet area (m^2)
C_{A1}	constant ($kg/s\ m^3$)
C_{A2}	constant ($kg/s^2\ m$)
C_d	discharge coefficient
d	piston diameter (m)
h	generic height in all clearances (m)
h_o	barrel, slipper, central clearance (m)
H	spherical journal clearance (m)
k_1	slipper constant (N/m^2)
l_i	length of a given land (m)
n	number of lands, including the grooves
p_i	general pressure (N/m^2)
p_{inlet}	pressure at the slipper central pocked (N/m^2)
P_{piston}	pressure inside each piston/cylinder chamber (N/m^2)
P_d	pump outlet pressure (N/m^2)
$p_{exter} = p_{tank}$	pump tank pressure (N/m^2)
Q_i	generalised flow (m^3/s)
Q_{exter}	leakage barrel plate towards the external radius (m^3/s)
Q_{inter}	leakage barrel plate towards the internal radius (m^3/s)
Q_{outlet}	total flow across the pressure relief valve (m^3/s)
$Q_{out\text{-}piston}$	output flow from each piston (m^3/s)
$Q_{slip\text{-}plate}$	leakage from each slipper (m^3/s)
$Q_{barrel\text{-}plate}$	leakage from barrel (m^3/s)
$Q_{piston\text{-}barrel}$	leakage from gap between piston and barrel (m^3/s)
Q_{sphere}	leakage from spherical bearing (m^3/s)
r	barrel, slipper generic radius (m)
r_m	average radius between land borders (m)
r_1	spherical journal internal radius (m)
R_P	piston pith radius (m)
t	generic time (s)
u	piston velocity (m/s)
v	flow generic velocity (m/s)
$\forall$	temporal volume of each piston (m^3)
$\forall_{valve+pipe}$	volume of valve, pipe and pump outlet together (m^3)
$\dot{\forall}$	flow piston-barrel per unit depth (m^2/s)
x	distance from the piston axis origin (m)
α	barrel, slipper tilt angle (rad)
γ	small groove angle (rad)
δ	sphere position angle (rad)
ε	swash plate angle (rad)
θ_b	barrel generic angular position (rad)
θ_i, θ_j	port plate pressure groove angular dimensions (rad)
θ_s	slipper generic angular position (rad)
θ_t	temporal angular position (rad)
μ	fluid dynamic viscosity ($kg/m\ s$)
ω_S	slipper spin (rad/s)
ω	pump turning speed (rad/s)

ripple was compared with the experimental one clarifying the effect of the timing grooves regarding the piston dynamics, they also optimized the timing groove length for a particular application.

Among the models presented, the one based on numerical data it can be expected to produce slow results, the others define leakages using very simple equations. In the present paper, an extensive set of explicit equations for every pump gap will be presented; all of the equations will be checked via performing a numerical analysis of the specified pump clearance. The equations will then be combined to study dynamically pump pressure ripple and leakages. The effect on the flow ripple when modifying the pump design will also be presented. Therefore in the present paper, a simulation model based on analytical

equations has been developed which produce very fast results and clarify very precisely the effect of different leakages through pump clearances.

2. Leakage on barrel plate

2.1. Previous studies

Considering relevant work regarding the barrel plate main characteristics, Helgestad et al. [11] studied theoretically and experimentally the effect of using silencing grooves on the temporal pressure and leakage fluctuation in one piston cycle. Triangular and rectangular silencing grooves versus port plate "ideal timing" and standard port plate were compared. For a range of operating conditions, the choice of triangular entry grooves was deduced to be the most appropriate. If the machine is required to turn in both directions, for example acting as motor, then groove symmetry will be required and rectangular grooves were deduced to be the most effective. They pointed out that the use of silencing grooves will modify the pump transient effects as well as the noise produced and the appearance of cavitation. The most appropriate opening angle and groove dimensions depend on the piston swept volume, swash plate angle, output pressure and rotational speed. Therefore each particular case has to be considered independently. The study considered the leakage at the slipper swash plate, evaluating the resistance effect of the slipper central hole.

Martin and Taylor [12] analysed in detail the start and finish angles for the pressure and tank grooves to have "ideal timing". As in [11] graphs were presented to understand the temporal pressure and flow in a single piston, leakage flow was not considered. The results showed that triangular silencing grooves were more appropriate in all cases except when the pump parameters were fixed; in such case "ideal timing" main grooves were desirable. The decrease of swash plate angle tended to reduce the pressure peak at the outlet groove entrance, while increasing reverse flow. Increasing the rotational speed increased the pressure peak at the outlet groove entrance.

Edge and Darling [13] presented an improved analysis able to evaluate piston temporal pressure and flow, the improvement being based on taking also into account the rate of change of momentum of the fluid during port opening. They found that the pump dynamics highly depend on the momentum change at the opening of the silencing groove. Although not considered in their study, they pointed out that inlet and delivery line impedance would have a significant effect on the line pressure fluctuations. The paper gives a good understanding of the piston pump problem, explaining carefully the effect of different silencing groove dimensions and shapes, including groove slope. As previous researchers before [11,12] they pointed out that triangular silencing grooves are the most appropriate for a piston pump operating over a wide range of working conditions. In regard of cavitation erosion, they define the most severe region at the end of the inlet port and at the start of the delivery port.

Jacazio and Vatta [14] studied the pressure, hydrodynamic force and leakage between barrel-plate. The study was mainly analytical using the Reynolds equation of lubrication and integrating it when considering pressure decay in radial direction and rotational speed. They found equations for the pressure distribution and lift force which showed the dependency of these parameters with turning speed.

Yamaguchi [15] demonstrated that a valve plate with hydrostatic pads allows a successful fluid film lubrication over a wide range of operating conditions. When analysing the barrel dynamics, the spring effect of the shaft was taken into account. Via changing parameters involved in the dynamic equations, such as dimensions, swash plate angle, friction coefficient, shaft spring constant, the most likelihood case of metal to metal contact between barrel and valve plate was considered.

Yamaguchi [16] studied experimentally the barrel plate dynamics; he used 4 different plates for experimentation, three of them with a groove and one without groove and no outer pad. He also worked with several fluids. To measure the film depth between barrel and plate, he used four position transducers located on the four axis of the plate. He found out that the gap barrel plate oscillated, the oscillation had two peaks a large one and a tiny one. For any kind of fluid used, it was found that the film thickness increased with inlet pressure. The amplitude of the fluctuation also increased with the pressure. No particular change in amplitude was recognized with the change in rotational speed. The amplitude of a plate with a groove was found to be larger than the amplitude of a plate without a groove. The leakage barrel plate was found as expected, to increase with pressure, although not linearly. For the plate without groove it was noticed that the effect of different fluid viscosities was almost imperceptible. He compared theoretical and experimental film thickness finding a good agreement.

Matsumoto and Ikeya [17] studied experimentally the friction, leakage and oil film thickness between the plate and cylinder for low speeds. It was deduced that the friction force was almost constant with rotational speed, but strongly depended on supply pressure and static force balance. The leakage was affected by supply pressure, rotational speed and static force balance. In a further paper, Matsumoto and Ikeya [18] focused more carefully on the leakage characteristics between cylinder block and plate, again the study was experimental and focused on low speed conditions. The results showed that, the fluctuation of the tilt angle of the barrel and the azimuth of minimum oil film thickness, depended mainly on change of the high pressure side number of pistons. The leakage flow rate fluctuation was "mainly caused by the accuracy of the motor shaft".

Kobayashi and Matsumoto [19] studied the leakage and oil film thickness fluctuation between the valve plate and barrel. They integrated numerically the Reynolds equation of lubrication when taken into account the pressure distribution in radial

and tangential direction, finding the flow, barrel tilt and barrel plate clearance versus the angular position. Very low rotation speeds were considered.

Weidong and Zhanlin [20] studied the temporal leakage flow between barrel and plate and piston and barrel, they studied separately the leakage on each barrel groove and the effect of the timing groove, barrel tilt and piston tilt were not taken into consideration.

Yamaguchi [21] gave an overview of the different problems found in tribology of pumps. When assessing the plate and cylinder block performance, he pointed out the effect of the leakage for different fluid viscosities when the valve plate had or had not a hydrodynamic groove (see also [22]). It was found that the use of a groove stabilizes the leakage for different fluid viscosities. Equations to determine the force, torques and accelerations versus the two main barrel axis were given as a function of the pressure distribution, which was found based on the Reynolds equation of lubrication.

One of the last research works on cylinder block is the one performed by Manring [23], where he evaluated the forces acting on the cylinder block and its torque over the cylinder main axis. To evaluate the force over the barrel due to the pressure distribution he considered the pressure distribution onto the pump outlet as constant and the decay along the barrel lands as logarithmic, independent on the barrel tilt and turning speed. He defined a tipping criterion based on the location of the reaction force over the barrel referred to the outer radius of the external land. Manring [24] also investigated various valve-plate slot geometries within an axial piston pump. The slot geometries had constant area geometry, linearly varying geometry and quadratic varying geometry. Manring found that a constant area slot design had the advantage of minimizing the required discharge area of the slot, the linearly varying slot design had the advantage of utilizing the shortest slot length, and the quadratic slot design had no particular advantages over the other two.

Ivantysynova et al. [7–9] using the numerical program CASPAR found the pressure distribution and the leakage between barrel–plate. Since the program considered the two-dimensional dynamic Reynolds equation of lubrication, the results obtained are highly precise, taking also into consideration heat transfer and therefore flow temperature variation.

In Bergada et al. [25] explicit equations based on the Reynolds equation of lubrication, were found to determine, leakage, pressure distribution, static and dynamic torques acting on the barrel, the barrel dynamics were particularly interesting and the theoretical results were matching the experimental ones found by Yamaguchi [16].

From all those studies it can be stated that barrel-plate clearance and leakage has been studied experimentally by Refs. [15–20] and analytically by Refs. [7–9,14], the effect of silencing grooves was undertaken by Refs. [10–13,24], the piston pressure-flow dynamics when leakage is not considered was presented in [10,12,13], very simple equations on leakage were used in [1,2,4] and piston dynamics when computed leakage in all pump gaps is considered was introduced in [6–8], but, despite the large amount of work done, the explicit equations considering the leakage barrel plate, were just introduced in previous research [25] undertaken by the present authors.

2.2. Mathematical analysis

In the present paper, the leakage and pressure distribution between the barrel and the port plate will be determined from the integration of Reynolds equation of lubrication in polar coordinates. The same method was used by Jacazio and Vatta [14], although in this paper, a more precise integration is undertaken. While taken tilt and rotation into account, assuming the flow is laminar and incompressible and moves in radial direction, the leakage barrel-plate can be given by Eqs. (1) and (2) as deduced in Bergada et al. [25]. Eq. (1) gives the main groove leakage towards the external barrel radius $r_{\text{exter}\,2}$ while Eq. (2) gives the main groove barrel/plate leakage towards the internal barrel radius $r_{\text{int}\,2}$, see Fig. 1

$$Q_{\text{exter}} = \frac{(p_{\text{tank}} - p_{\text{d}})}{12\mu \ln\left(\frac{r_{\text{exter}}}{r_{\text{exter2}}}\right)} \begin{bmatrix} h_0^3[\theta_{\text{b}}]_{-\theta_i}^{\theta_j} + 3h_0^2\alpha r_{m\,\text{exter}}[\sin\theta_{\text{b}}]_{-\theta_i}^{\theta_j} + 3\,h_0\alpha^2\, r_{m\,\text{exter}}^2 \\ \left[\frac{1}{4}\sin(2\theta_{\text{b}}) + \frac{\theta_{\text{b}}}{2}\right]_{-\theta_i}^{\theta_j} + \alpha^3 r_{m\,\text{exter}}^3\left[\frac{1}{12}\sin(3\theta_{\text{b}}) + \frac{3}{4}\sin\theta_{\text{b}}\right]_{-\theta_i}^{\theta_j} \end{bmatrix}, \tag{1}$$

$$Q_{\text{inter}} = -\frac{(p_{\text{tank}} - p_{\text{d}})}{12\mu \ln\left(\frac{r_{\text{inter}}}{r_{\text{inter2}}}\right)} \begin{bmatrix} h_0^3[\theta_{\text{b}}]_{-\theta_i}^{\theta_j} + 3\,h_0^2\alpha r_{m\,\text{inter}}[\sin\theta_{\text{b}}]_{-\theta_i}^{\theta_j} + 3h_0\alpha^2\, r_{m\,\text{inter}}^2 \\ \left[\frac{1}{4}\sin(2\theta_{\text{b}}) + \frac{\theta_{\text{b}}}{2}\right]_{-\theta_i}^{\theta_j} + \alpha^3 r_{m\,\text{inter}}^3\left[\frac{1}{12}\sin(3\theta_b) + \frac{3}{4}\sin\theta_{\text{b}}\right]_{-\theta_i}^{\theta_j} \end{bmatrix}. \tag{2}$$

The total leakage barrel-plate will be the addition of the two leakage flows. According to Eqs. (1) and (2), leakage barrel plate will depend on the geometry, internal and external pressures, tilt, and the central clearance. Leakage due to the timing groove should also be included, but an analysis presented in Bergada et al. [25] shows that such leakage is insignificant when compared to the main groove one and therefore will be neglected.

2.3. Comparison between analytical and numerical results for barrel-plate leakage

In order to validate the analytical leakage equations, a numerical model for the barrel-plate clearance based on Reynolds equation of lubrication was developed. A finite difference technique was used for Discritization. Further details on the numerical model developed can be found in Bergada et al. [25]. Fig. 2 represents, for a set of different central clearances, the comparison between the leakages calculated from Eqs. (1) and (2) and from the numerical model developed in [25], 10 and 25 MPa pump pressure. A perfect agreement between equations and numerical results are found for all cases studied.

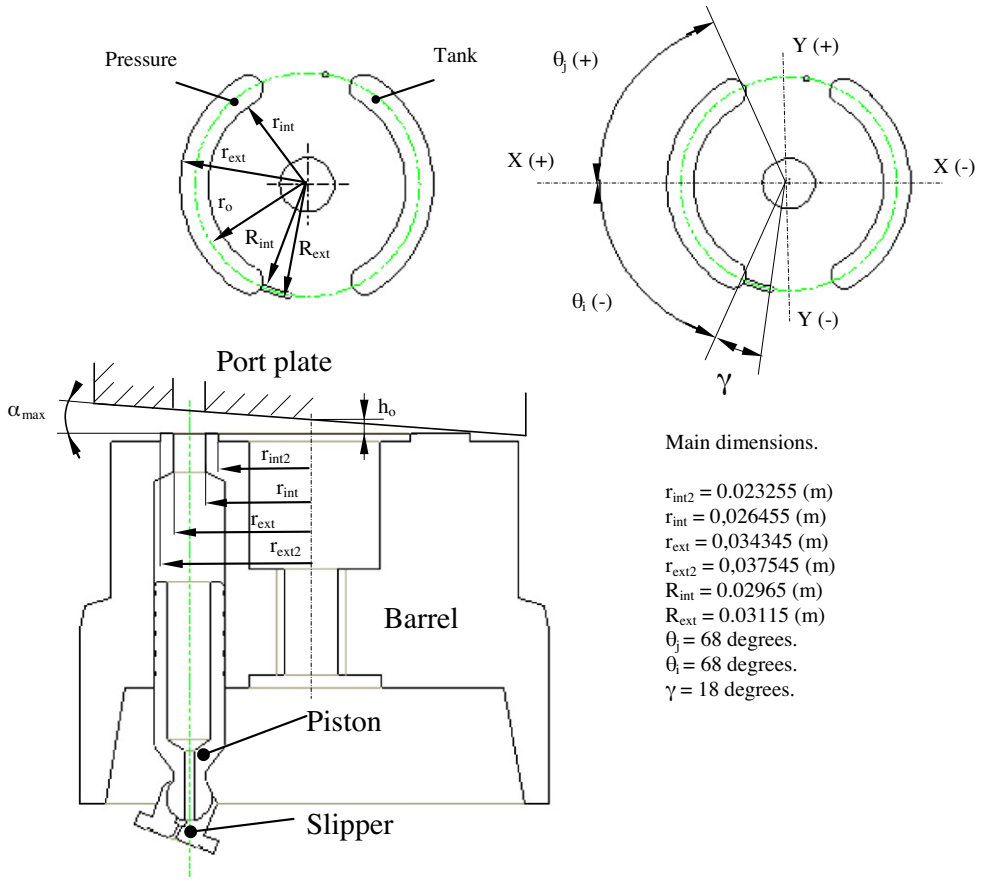

Fig. 1. Barrel-plate configuration.

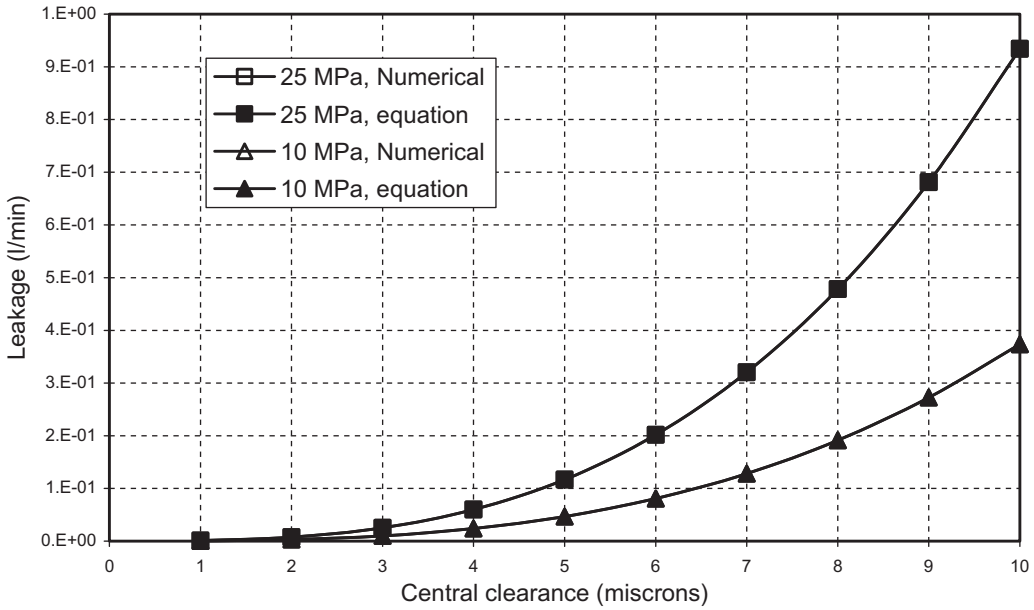

Fig. 2. Leakage barrel-plate versus different central clearances and maximum alpha at each clearance, different inlet pressures.

3. Leakage slipper–swash plate

3.1. Previous research

There has been many publications in this general subject area over the last 40 years and concerned with improving the performance of piston pumps and motors. For example Fisher [26] studied the case of a flat slipper with single land on a rotating plate. Both cases, when the slipper was parallel and tilted with respect to the swash plate were considered, the load capacity, restoring moment, and flow characteristics were studied. Fisher demonstrated that if a flat slipper tilts slightly so that the minimum clearance occurs at the rear; the hydrodynamic loads generated tend to return the slipper to the non tilted position. Fisher concluded that when the ratio of the angle of tilt to the angle at which the slipper would just touch the plate is higher than 0.675 then slipper equilibrium would be impossible since the load plus the dynamic force cannot be balanced by the hydrostatic force.

Böinghoff [27] performed a deep study on slippers. He studied theoretically the static and dynamic forces and torques acting on a single piston, via analyzing carefully the slipper performance as it rotates around the swash plate, he also took into account the torque generated on the spherical bearing. Large quantities of experimental results where also generated, in which torque and leakage were evaluated for different position angles, and low turning speed. The effect of oil viscosity on the torques created was also taken into account. Pump leakage was studied for different swash plate angles and turning speeds. Leakage was found to be smaller at low speeds <5 rad/s, and low swash plate angles, and increased with turning speed. He also studied experimentally the influence of slippers with different lands, focusing on torque and leakage at different turning speeds. It must be pointed out that although the slipper studied had four lands, just one of them can be considered as full land, the rest were vented. He found that the torque remained almost constant with turning speed when 1 or 2 lands were used, and quickly increasing with speed when using four lands. Leakage was found to be lower when decreasing the number of lands, and for speeds higher than 10 rad/s.

Hooke and Kakoullis [28] showed that a degree of non-flatness was essential to ensure the successful operation of the slipper, and the non-flatness must have a convex profile. They concluded that the lift contribution due to spin, had a second order effect. The centripetal forces resulting from the speed of the pump had a tendency to tilt the slipper outwards thus reducing the clearance on the inside of the slipper path. They also pointed out that the friction on the piston ball played a major role in determining the behaviour of the slipper. In a further paper Hooke and Kakoullis [29] studied more carefully the couples created by the slipper ball, finding that the major source of variation between slippers did not arise from differences on surface profile but from differences in the friction in the ball-cup and piston-cylinder pairs. He concluded that ball-cup friction increased with pressure, and contact metal to metal was likely to appear when lubrication was deficient.

Iboshi and Yamaguchi [30,31], working with single land slippers, found a set of equations based on the Reynolds equation of lubrication which gave the flow and the main moments acting on the slipper; the slipper displacement velocity and tilt were considered in the theory. They found that there was a limit of fluid film lubrication for the specific supply pressure and rotational speed. They also defined a diagram checking the conditions under which metal to metal contact on the slipper may appear. It was pointed out that the friction of the spherical bearing affects significantly the tilt angles, and the rotational speed affects the central clearance of the slipper plate. Experimentally they found that the slipper plate clearance, under steady rotational conditions, was fluctuating.

Hooke and Kakoullis [32] studied more carefully the effect of non-flatness and the inlet orifice on the performance of the slipper. They gave a very good explanation of the equations used and the mathematical process to find them, finding the moments along the two main axes of the slipper. They found out that between 2% and 5% of the load was being supported by hydrodynamic forces, and tilt was necessary to produce the desired hydrodynamic lift. It was also found that the increase of the film thickness with reduction of slipper non-flatness was very small. In all geometrical conditions studied, it was found that slippers with no inlet orifices had larger clearances than slippers with orifices; however starvation effects and cavitation may appear. In [33] Hooke and Li focused on the lubrication of overclamped slippers, the clamping ratio being defined as the relation between the hydrostatic lift acting on the slipper and the piston load. Typical overclamped ratios ranged between 1% and 10%. They noticed that to have successful slipper lubrication, the plate where the slipper slides must be well supplied with fluid. The tilt was found to be proportional to the non-flatness magnitude divided by the square root of the slipper central clearance. In this paper the Reynolds equation of lubrication for tilted slippers had been integrated numerically. In [34] Hooke and Li analysed carefully the three different tilting couples acting on slipper, finding that the tilting couple due to friction at the slipper running face, is much smaller than the ones created at the piston-cylinder, piston-slipper interfaces, and the centrifugal one. All slippers tested had a single land. The slippers were found to operate relatively flat, clearances were highly dependent on the offset loads, and the minimum clearance was found to be not particularly sensitive to the type of non-flatness magnitude.

Takahashi and Ishizawa [35] studied the unsteady laminar incompressible flow between two parallel disks with the fluid source at the centre of the disks. Both the flow rate and the gap between disks were varied arbitrarily with time and independently of each other. The Navier–Stokes equations were solved via expanding the variables in series, the technique of asymptotic series expansion in the radial direction was used, and on the basis of a new theory of multifold series expansion. The theory presented gave light to the study of the complicated characteristics of the inertial forces. Li and Hooke [36] studied the lubrication of composite slippers on water based fluids. It was found out that the slipper plate

clearance was smaller than when using hydraulic oil and it was essential that the surfaces of the slipper and plate should be highly polished in order to accomplish a successful slipper operation. Even for the best material combinations, problems were encountered when the system was run at high fluid pressures and low running speeds. When turning at speeds lower than 300 rpm, contact at the slipper plate was found. The slipper plate clearance increased when increasing the slipper surface.

Koc et al. [37] focused their work on checking whether underclamped flat slippers could operate successfully or whether a convex surface was required. A good understanding of the three couples acting on the slipper, previously defined by Hooke et al. [29,34], was essential. They took into account the work done by Kobayashi et al. [38] on the measurements of the ball friction. They concluded that polishing of the running face of the slipper to a slightly convex form, appeared to be essential for successful operation under all conditions. It was also found that the insertion of an inlet orifice at the centre of the slippers had in all cases the effect of increasing the central clearance, though tending to destabilise the slippers. Notice that the insertion of an inlet orifice seams to give opposite effects in Refs. [32,37]. It must be bared in mind that in Ref. [32] the slipper used was having conical lands, while in Ref. [37] the sliding surface is slightly convex. The size of the central orifice in underclamped slippers appeared to be most critical for a successful operation. Harris et al. [39] created a mathematical dynamic model for slipper-pads, in which lift and tilt could be predicted, the model was able to handle the effect of the possible contact with the swash plate. The simulation showed that slipper tilt was much higher at suction that at delivery and at delivery tilt increased with pump speed.

In [40,41] Koc and Hooke studied more carefully the effects of orifice size, finding that the underclamped slippers and slippers with larger orifice sizes run with relatively larger central clearances and tilt more than those of overclamped slippers with no orifice. Slippers with no orifice had greatest resistance to tilting couples and the largest minimum film thickness. One of the major effects of the orifices was to greatly reduce the slipper resistance to tilting couples. They pointed out that the use of two lands, an inner and outer land, brought more stability to the slipper. They also indicated that when a slipper incorporates a second land, the space between lands needs to be vented to avoid the generation of excessive hydrostatic lift, allowing the flow trapped between lands to escape. The direction and magnitude of the tilt was found to be directly dependent on the offsets imposed.

Tsuta et al. [42] analysed in detail the slipper dynamics in a piston pump. As other authors before [26,30] Tsuta used the Reynolds equation of lubrication considering slipper spin, tangential velocity over the pump axis and angular and radial pressure distribution. The differential equation was solved via expanding it in power series, finding the coefficients of some of the first terms of the series. The pressure distribution given in the power series was later used to find out the force and torques over the slipper. Slipper dynamics was based on such information.

Wieczoreck and Ivantysynova [43] developed a package called CASPAR which used the bidimensional equation of lubrication and the energy equation in differential form. It was shown how transient cylinder pressure could be computed; when considering the leakages between piston and cylinder, slipper and swash plate, and barrel and port plate. In addition, the clearance and tilt of the slipper was shown to vary over one revolution of the pump, a single land slipper plate was used in the theoretical and experimental analysis.

From all these papers it can be seen that although research on slippers has been long and deep, no work has been performed on slippers with non vented grooves, although first attempts to understand grooved slippers behaviour were developed by Böinghoff [27] and Kakoulis [44], although in both cases the grooves were vented.

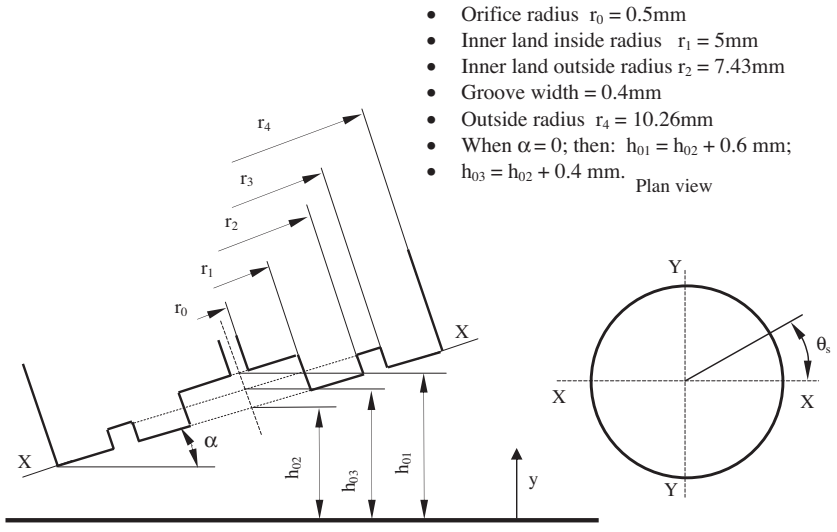

Fig. 3. Tilt slipper main parameters.

3.2. Mathematical analysis

The main dimensions of the slipper analysed in this paper are given in Fig. 3, notice that the slipper has a non vented groove located at the centre of the land. The basis of the theory to find out the pressure distribution below the slipper, the leakage slipper swash plate and the torque generated, under static conditions, was given in Bergada et al. [45,46]. The following assumptions were made in order to determine the set of equations for the slipper–swash plate leakage.

1. Flow will be considered laminar in all cases.
2. The slipper plate clearance is not uniform; the slipper is tilted.
3. Steady conditions are considered.
4. Slipper spin is taken into account.
5. Flow will be radial at the slipper face.

When taking into account the above assumptions, the leakage slipper- swash plate can be given by Eq. (3) as described in Bergada et al. [45]. Due to the complexity of the resulting integral, Eq. (3) needs to be integrated numerically

$$Q_{\text{Slip-plate}} = -\int_0^{2\pi} \frac{k_1}{12\mu}\,\mathrm{d}\theta_s, \tag{3}$$

where,

$$k_1 = \frac{p_{\text{tank}} - p_{\text{inlet}} - \frac{3\mu\omega_S\,\alpha\sin\theta_s}{2}\left[\sum_{i=1}^{i=n}\frac{r_{m\,i}(r_{i-1}^2 - r_i^2)}{(h_{0i}+\alpha r_{m\,i}\cos\theta_s)^3}\right] - 3\mu\omega_S\alpha\sin\theta_s\left[\sum_{i=1}^{i=(n-1)}\frac{\ln\left(\frac{r_{i+1}}{r_i}\right)\left[\sum_{j=1}^{j=i} r_j^2(r_{m(j+1)} - r_{mj})\right]}{(h_{0(i+1)}+\alpha r_{m(i+1)}\cos\theta_s)^3}\right]}{\sum_{i=1}^{i=n}\frac{\ln\left(\frac{r_i}{r_{(i-1)}}\right)}{(h_{0i}+\alpha r_{mi}\cos\theta_s)^3}}. \tag{4}$$

Notice that the parameter k_1, Eq. (4), is given in generic form, being "n" the number of slipper lands, including the grooves and the slipper central pocket. For the present slipper, the number of lands is four, since the slipper under study has the central pocked, a first land, the groove and a second land. Therefore Eq. (4) will need to be defined for the slipper under study and then substituted in Eq. (3).

3.3. Comparison between analytical and numerical results for slipper-plate leakage

In order to validate the analytical leakage equations, a numerical model has been formulated by integration of Navier–Stokes equation over a boundary fitted grid via Finite volume technique. The Navier–Stokes equation has been transformed from physical domain to computational domain in order to have orthogonal grid. The transformed momentum equations are coupled with continuity by using Semi Implicit Pressure Correction method. Further details regarding the development of the numerical model can be found in the 3rd chapter of Kumar PhD thesis [47].

In Fig. 4 is presented the leakage for a tilt slipper with groove, again numerical and analytical results are being compared. Notice that the leakage found by the equations is, for the highest tilts studied, about 5% bigger than the one found via using

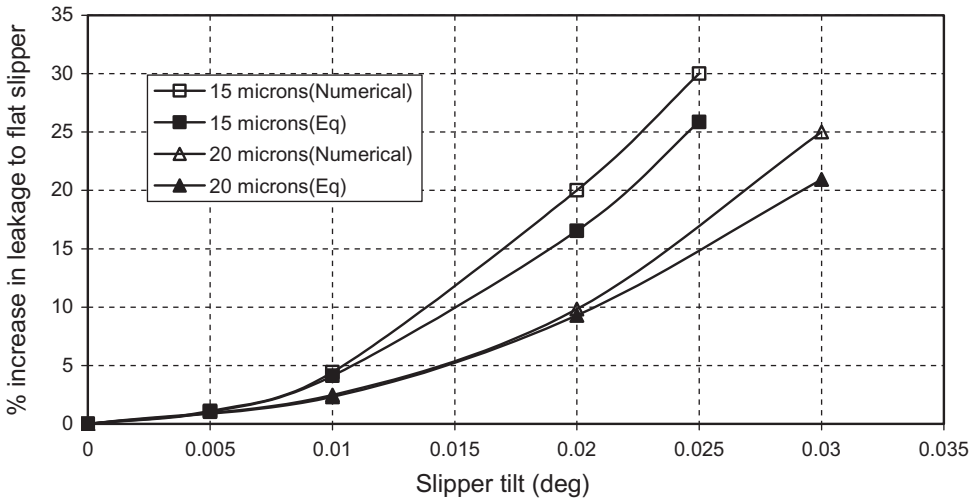

Fig. 4. Leakage between the slipper-swash plate clearance, comparison CFD and equations.

CFD, such differences can be explained when understanding that the Navier–Stokes equation takes into account the pressure distribution along the tangential direction, and such distribution is specially relevant inside the groove, then an smaller pressure differential between the central land and groove, will bring an smaller flow. It is important to notice that, the equations produce very good results for leakage between slipper and plate at low tilts, smaller than (0.01°) and in literature has been found that slipper tends to run at very small tilts, therefore using the analytical equations rather than the numerical model does not introduce much error in slipper leakage and produce much faster results.

It has to be pointed out that, the slipper leakages presented in Fig. 4 have been calculated when slipper is in static conditions with respect to swash plate, as the dynamics effect of slipper can not be considered by the analytical equations (3) and (4). On the other hand it has been presented in Kumar et al. [48] that the rotation of slipper does not have any net effect on leakages when slipper is running parallel to swash plate, although under tilted conditions, leakage does depend on tilt [47]. In the present paper, a very low value of (0.01°) on slipper tilt was considered; therefore the leakage given by the analytical equations is fully trustable, even though slipper dynamics is not considered in the analytical equations.

4. Leakage between piston and barrel

4.1. Previous research

To evaluate leakage in spools and pistons, it is traditionally used Poiseulle equation when there is no relative movement and Couette–Poiseulle equation when relative movement exist. Pistons, in piston pumps and motors, often have several grooves cut along the axis in order to increase stability, decrease friction and reduce lateral forces. Some attempts have been pursued to find the flow and pressure distribution theoretically taking into account the effect of groves; Milani [49] applied continuity equation to link the Poiseulle equation in each land, and considered that pressure in each groove will be constant. The same method was used by Borghi et al. [50,51], although they applied it to a single groove tapered spool. In both cases relative movement between piston and cylinder was not considered, yet eccentricity was taken into account. In any case, the most precise way to find out the leakage and pressure distribution would be via using the two dimensional Reynolds equation of lubrication. The main difficulty here is that the equation needs to be integrated using a finite difference method or another appropriate method. Such work, although when grooves were not considered, was undertaken by Ivantysynova et al. [5,9] which found the dynamic pressure distribution and leakage between piston and barrel considering piston tilt, piston displacement and head transfer. Elasto-hydrodynamic friction was also considered.

In the present study, a direct method to find out the pressure distribution and leakage in the piston/cylinder gap will be described. The advantage of this new method is that the relative movement of the piston cylinder is taken into account, and also groove effect is considered. The disadvantage is that the eccentricity effect cannot be considered.

4.2. Mathematical analysis

For this particular case, the equations about to be presented are based on the one-dimensional Reynolds equation of lubrication, the Couette–Poiseulle equation, and the continuity equation. The full description of the mathematical analysis is to be found in Bergada and Watton [52], in what follows just the final leakage equation will be presented, the mathematical development is to be found in Appendix 1. The assumptions considered for this case are:

1. Laminar flow is being considered in all cases.
2. The flow is two-dimensional.
3. Relative movement between piston and barrel exists.
4. The gap piston cylinder is simulated as the gap between two flat plates.
5. No eccentricity is considered.
6. Each land and groove is modelled as a flat plate.

The piston main dimensions are (see Fig. 5):

$h_1 = h_3 = h_5 = h_7 = h_9 = h_{11} = 2.5\ \mu m.$
$h_2 = h_4 = h_6 = h_8 = h_{10} = h_1 + 0.4\ mm.$
$L_1 = 1.42\ mm.$
$L_{11} = 19.5\ mm.$
$L_2 = L_4 = L_6 = L_8 = L_{10} = 0.88\ mm.$
$L_3 = L_5 = L_7 = L_9 = 4\ mm.$

The leakage across the piston-barrel gap can be given by Eq. (5) which has been developed by the integration of one dimensional Reynolds equations by taking into account the above specified assumptions.

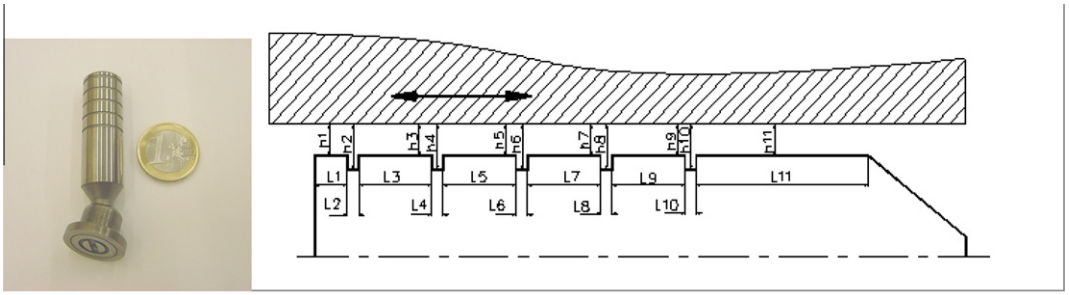

(a) Piston layout. (b) Piston geometry

Fig. 5. Piston slipper assembly.

$$q_{\text{piston-barrel}} = \pi d\left[\frac{h_1 R_p \tan\varepsilon(-\sin(\omega t))\omega}{2}\right] - \frac{\pi d}{12}\left[\frac{P_{\text{tank}} - P_{\text{piston}} - 6R_p \tan\varepsilon(-\sin(\omega t))\omega\mu\left[\frac{h_{10}-h_1}{h_{10}^3}\right](l_2+l_4+l_6+l_8+l_{10})}{\frac{\mu}{h_{11}^3}(l_1+l_2+l_3+\cdots+l_{11}-\frac{l_{11}}{2}-R_p\tan\varepsilon\cos(\omega t))+\mu\left[\left(\frac{1}{h_2^3}-\frac{1}{h_1^3}\right)(l_2+l_4+l_6+l_8+l_{10})\right]}\right]. \quad (5)$$

Eq. (5) gives the dynamic leakage piston-cylinder for any given swash plate angle and considering the dimensions of the five grooves cut on the piston, also the temporal length of the piston inside the cylinder is considered.

4.3. Comparison between analytical and numerical results for piston-barrel leakage

A Reynolds equation based model has been formulated in order to validate the analytical piston-barrel leakage. The bi-dimensional Reynolds equation of lubrication has been integrated using a control volume formulation over uniform orthogonal grid. The numerical model is capable of taking into account the piston eccentric displacement, piston tilt with cylinder axis and piston cylinder relative movement. Further details on the numerical model can be found in Kumar [47].

Fig. 6 presents a comparison between analytical and numerical leakage for piston-cylinder clearance at 1000 rpm pump turning speed, 10 μm central clearance, 30 and 10 MPa inlet pressure. Notice that pressure variation affects the leakage just when the piston moves from the LDC (lower death centre) to the UDC (upper death centre). The figure shows a very good agreement between numerical and analytical results.

It is important to point out that piston eccentricity can not be considered when calculating leakage using the analytical equation (5), but it has already been proven by numerical analysis in Kumar [47] that in the presence of grooves, piston eccentric displacement does not effect the leakage as long as a fix central clearance is maintained between piston and cylinder. Therefore Eq. (5) produces very good results for leakage in the piston-cylinder clearance under all working conditions.

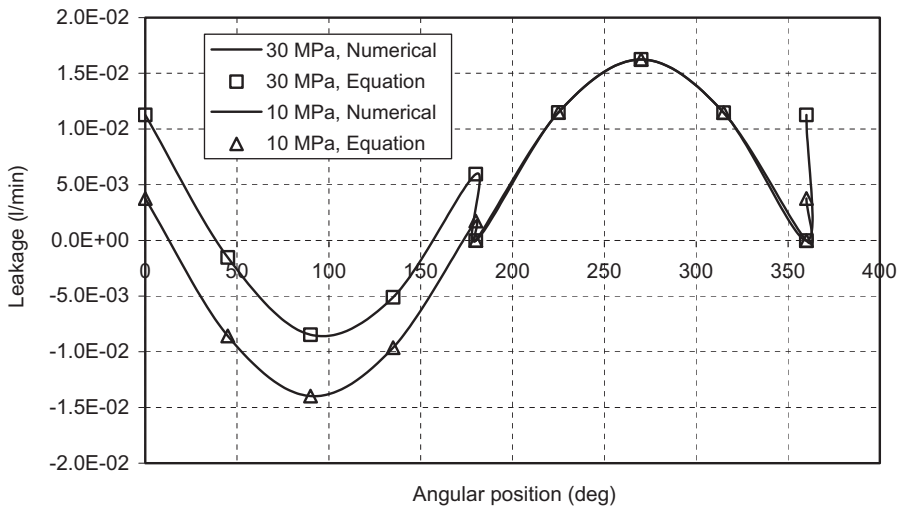

Fig. 6. Leakage between piston cylinder clearance versus angular position at 1000 rpm pump turning speed, 10 μm central clearance, two different inlet pressures, comparison between numerical and equation.

5. Leakage spherical piston–slipper bearing

5.1. Previous research

Spherical journal bearings in piston pumps have been studied in some depth, mainly the different researchers focused on studding the friction piston ball–slipper. Böinghoff [27] performed a first analytical study on the spherical bearing friction. Hooke and Kakoullis [28] pointed out that friction on a piston-slipper spherical junction plays a major role in determining the behaviour of the slipper. Later Hooke and Kakoullis [29] studied experimentally the couples acting on the piston-slipper spherical junction, they concluded that lubrication is under all conditions deficient, appearing metal to metal contact. Friction increases with pressure and small slipper plate tilt angles. Friction on the spherical junction causes the piston to rotate. In [30,31] Iboshi and Yamaguchi pointed out that friction on the spherical bearing affected significantly the slipper tilt angles, rotational speed affects the central clearance slipper-plate. It must be said that these results agree very well with Hooke's considerations.

In [34] Hooke and Li analyzed carefully the three different tilting couples acting on the slipper, finding that the tilting couple due to friction at the slipper running face is much smaller than the ones created at the piston – cylinder, piston – slipper interfaces.

Kobayashi et al. [38] studied experimentally the friction torque characteristics between the piston ball and the slipper. Different surface coatings, clearances and surface roughness were analyzed. They found that friction torque increased with the pressure, tending to an asymptotic value, an increase on the swash plate angle created a decrease on the friction torque, the friction torque decreased as clearance increased; there was also a slight decrease on friction torque with increase of oil temperature. Regarding the materials, they found that the use of PST05 solid lubricant witch was coated with PTFE gave the lowest friction torque at all pressures. The use of different surface roughness did not prove any significant change on friction torque. The measurements on leakage showed a small leakage decrease when increasing slipper spin.

Spherical bearing was also experimentally studied in a ball-piston pump by Abe at al. [53,54], the work was mainly focused on the friction coefficient, although piston velocity, and pressure contact between sphere and cam were also evaluated, they had a first attempt on explaining pressure distribution on the spherical bearing. Different shapes of pistons with restricting holes were evaluated.

Elastohydrostatic lubrication of piston balls and slipper bearings was studied by Kobayashi and Ikeya [55], in fact, most of the work was focused in presenting the slipper swash plate gap and the leakage as a function of the slipper main land length and the slipper central hole. It was found that minimum film thickness and leakage through slipper tended to reach an asymptotic value with the increase of the slipper land length.

The transformed Reynolds equation of lubrication in spherical coordinates was accomplished by Meyer [56], the integration of such equation gives the pressure distribution along the spherical journal bearing.

5.2. Mathematical analysis

From all the studies undertaken until now, it can be stated that most of the work done on spherical bearings is related to friction torque, some attempts in evaluating pressure distribution and leakage were carried out experimentally by Abe et al. [53], recently Meyer [56] presented the transformed Reynolds equation of lubrication in spherical coordinates, the integration giving the pressure distribution along the spherical bearing. Nevertheless, and due to the lack of information especially on the leakage thorough a spherical journal bearing it was decided to develop the following equations. It must be bared in mind that the leakage between the piston and slipper spherical bearing is expected to be small compared with the slipper-swash plate or the barrel-port plate ones. However it is interesting to develop the equations, then a thorough evaluation of the piston pump can be performed.

For the pump under study, the spherical journal main dimensions are (see Fig. 7):

$r_1 = 5.5$ mm.
$H = 2.54$ μm.
$\delta_1 = 10.47°$.
$\delta_2 = 125.09°$.

The leakage through the spherical journal can be found via integrating the transformed Reynolds equation of lubrication in spherical form (Eq. (6)) found by Meyer [56], assuming a spherical journal without rotation, steady state conditions and distance between the two spheres as constant, the resulting equation is:

$$\frac{\partial}{\partial\delta}\left(h^3 \sin\delta \frac{\partial p}{\partial\delta}\right) = 0 \quad \text{for } \delta_1 < \delta < \delta_2. \tag{6}$$

The boundary conditions needed to solve this differential equation are:

$$\begin{aligned} &\delta = \delta_1 \Rightarrow P = P_{\text{inlet}}, \\ &\delta = \delta_2 \Rightarrow P = P_{\text{tank}}. \end{aligned} \tag{7}$$

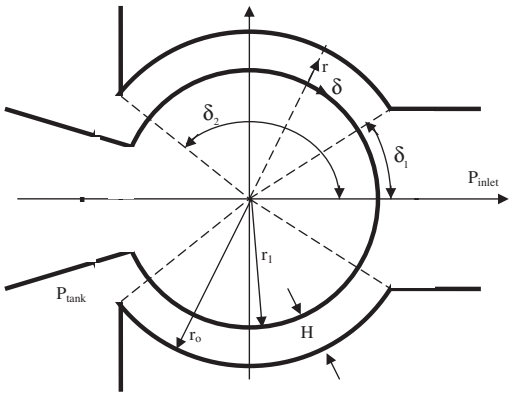

Fig. 7. Spherical bearing piston-slipper.

Assuming flow between two flat plates as Poiseulle flow, the volumetric flow will be given as:

$$dQ = \int_0^H -\frac{1}{\mu}\frac{dP}{dz}\frac{r}{2}(H-r)2\pi(r_0+r)\sin\delta dr. \tag{8}$$

The relation between the angle differential and the arc differential is:

$$dz = (r_1 + \frac{H}{2})d\delta. \tag{9}$$

The first integration of Eq. (6) and once the constant of integration will be found, has to be substituted in Eq. (8) once taken into consideration Eq. (9). Then, the leakage across the spherical bearing can be given as:

$$Q_{\text{sphere}} = \frac{(P_{\text{inlet}} - P_{\text{tank}})\pi(r_1\frac{H^3}{6} + \frac{H^4}{12})}{\mu(r_1 + \frac{H}{2})\ln\left[\frac{tg\frac{\delta_2}{2}}{tg\frac{\delta_1}{2}}\right]}. \tag{10}$$

A more detailed development to find out the expressions giving pressure distribution and leakage in a spherical journal can be found in Watton [57].

6. Flow leaving each piston-barrel chamber

Since the area through which the flow is leaving each piston-barrel chamber is much bigger than the rest, the flow is traditionally assumed as turbulent, for such cases the conventional equation used is:

$$Q_{\text{out-piston}} = \text{sign}(p_{\text{piston}} - p_d)C_d A_c\sqrt{\frac{2}{\rho}|p_{\text{piston}} - p_d|}. \tag{11}$$

The discharge coefficient is generally assumed as constant and equal to 0.6 although in reality depends on the cross sectional area and pressure differential. The temporal cross sectional area (A_c) has been calculated for each piston to its corresponding position. Fig. 8a presents the top view schematic diagram of all nine pistons assembly, showing the barrel plate slots and its angular dimensions. The area, across which the output flow leaving the piston-barrel chamber in direction pump outlet will exist, is represented in Fig. 8b. Notice that due to the entrance timing groove, the area increase has two different slopes.

It is noticed that the output area across which the flow towards the pump output will leave, goes from zero to a maximum every 165°. When a piston enters in contact with the timing groove, the output area increase rather sharply, and once the piston enters in contact with the main groove, the area increases in a lower rate. While the piston is fully in contact with the main groove, the output area remains constant. When calculating the temporal timing groove area, it should also be considered the timing groove depth, since the input area is in reality the cross sectional area perpendicular to the fluid flow. For the present pump the timing groove depth is constant at all points and has a value of 1 mm.

7. Temporal piston cylinder differential equation

As the barrel turns around the swash plate, the volume of each piston-cylinder chamber and the area of its connecting side to the pump output changes with time. The connecting side area of each piston as a function of the angular position can be seen in Fig. 8. The temporal volume of each piston-cylinder chamber as a function of swash plate angular position is given by Eq. (12)

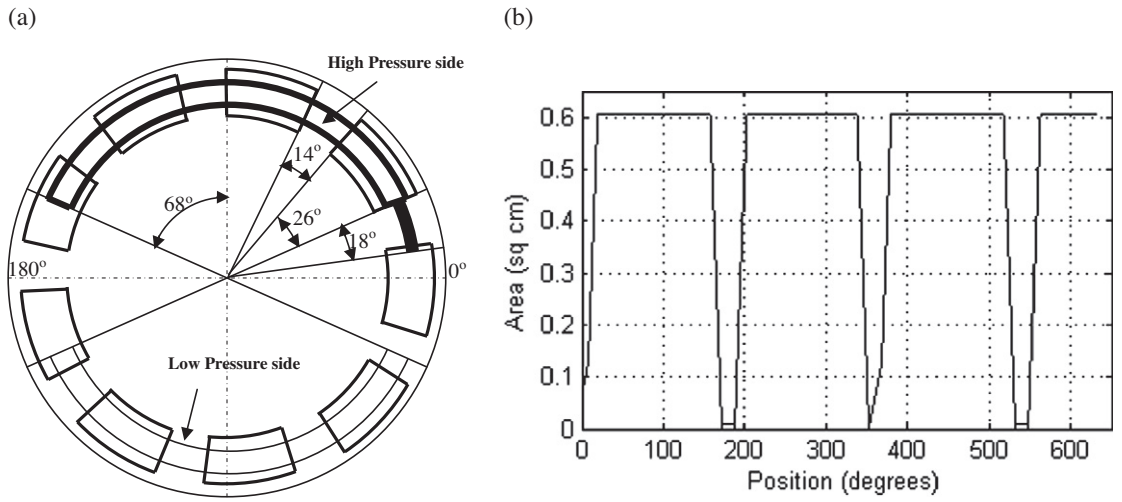

Fig. 8. Temporal cross section area (A). (a) Barrel/port plate view. (b) Single piston/port plate temporal area.

Table 1
Leakages and out flow at different clearances, set valve pressure 10 MPa.

	Clearances (μm)	%Flow	Clearances (μm)	%Flow	Clearances (μm)	%Flow
Barrel-plate	5	71.4	10	70	5	26.04
Slipper	5	22.5	10	23.9	10	71.64
Piston	5	2.7	10	2.7	5	1.04
Spherical bearing	5	3.4	10	3.4	5	1.28
Total leakage	0.609% of total output flow		4.57% of total output flow		1.63% of total output flow	

$$\forall = \forall_0 + \frac{\pi d^2}{4} R_p \tan\varepsilon(\cos\theta_t - 1), \tag{12}$$

where $\forall_0$ is the cylinder volume when the piston is located at the bottom dead centre.The temporal pressure inside each piston can be found by applying continuity equation in integral form in the piston-cylinder chamber, as given in Eq. (13)

$$\frac{dp_{piston}}{dt} = \frac{\beta}{\forall}\left(-Q_{slip\text{-}plate} - Q_{barrel\text{-}plate} - Q_{sphere} - Q_{piston\text{-}barrel} - Q_{out\text{-}piston} - \frac{d\forall}{dt}\right). \tag{13}$$

Eq. (13) gives the temporal pressure inside the piston-cylinder chamber as a function of the flow leaving the chamber, the fluid bulk modulus and the temporal volume of the chamber. According to Ma et al. [10], the flow due to the fluid inertia when entering the timing groove, should also be included in Eq. (13), reminding that in the present case the timing groove has a constant depth, such small flow has been calculated, but under all conditions studied such flow was over 10 times smaller than the spherical leakage, which is by far the smallest leakage in the pump, as it will be presented in Table 1. Therefore such leakage inertia effect has not been included in Eq. (13), since it is negligible.

Once all leakage equations are being substituted in Eq. (13) and after integration is performed, the time dependent pressure distribution inside one piston-cylinder chamber and the time dependant leakages through all pump gaps can be evaluated.

8. Temporal outflow ripple, combination of nine pistons

In order to study the effect of the nine pistons regarding the entire pump dynamics, it was decided to apply the continuity equation in integral form. When combining the output flow from all the pistons connected to higher pressure side at any time instant, it results in Eq. (14)

$$\frac{dp_d}{d\theta_t} = \frac{\beta}{\omega\forall_{valve+pipe}}\left(\sum_{i=1}^{n} Q_{out\text{-}piston} - Q_{outlet}\right), \tag{14}$$

n = number of pistons connected to the pump outlet at any time.

Notice that in Eq. (14) the volume considered is the one involving the output port of the pump, the volume of the tube connecting the pump and the relief valve, and the volume of the relief valve, volume submitted under pressure.

The flow leaving the pump, will have to pass though the pressure relief valve, the relation between this flow, the pressure differential between relief valve inlet and outlet and the valve cross section is given in Eq. (15)

$$Q_{\text{outlet}} = \text{sign}(p_d - p_{\text{tank}})\, C_d A_{\text{valve}} \sqrt{\frac{2}{\rho}|p_d - p_{\text{tank}}|}. \tag{15}$$

The relief valve dimensions and its dynamics, do affect the pump output flow/pressure ripple, it is therefore necessary to consider the relief valve dynamics in order to include its behaviour when studding the overall pump behaviour. For the present study, the valve cross section was calculated for each working condition and substituted in Eq. (15).

9. Computational technique

Fig. 9 shows a combined flow assembly of all the pistons under pressure. Pistons numbered from 1 to 5 are connected to high pressure side and pistons numbered from 5 to 9 are connected to tank side. Piston 5 is shown twice, as it can be connected to high pressure side or tank side depending on barrel angular position. Notice that, the total pump leakage is the addition of barrel leakage, the slipper-plate, piston-barrel and spherical bearing leakages coming for each of the nine pistons at any given time. It can also be seen that pump outlet flow is the addition of the flow, coming from the pistons connected to the high pressure side. The rectangular box connecting pump outlet with the pressure relieve valve, represents the total volume of valve, pipe and pump outlet port.

A computer program has been written in MATLAB to combine all Eqs. (1), (2)–(15) according to the flow chart shown in Fig. 9. First the contact area (A_c) for each piston corresponding to its position has been determined and then leakages through all four clearances have been calculated for all nine pistons. For the first time step, the pressure inside the piston chambers connected to high pressure side is assumed to be the given initial pressure condition. After that, all nine pistons have been combined using Eq. (14), finding the output pressure (P_d) when advancing in time. This calculated output pressure (P_d) provides the pressure just outside piston chamber (pump outlet) for the next time step. The numerical integrations have been performed by using fifth order Runge–Kutta method.

10. Experimental setup

In order to find out the dynamic pressure ripple inside the piston-cylinder chamber, the test rig presented in Fig. 10 was created in Cardiff University. Three very high response Kistler pressure transducers were located in cylinders 1, 4 and 7, Fig. 10a shows two of the transducers already in position. Notice that the connecting cables are coming out of the pump through the pump axis. Since the entire system, barrel, transducers and pump axis, turn, a slip ring assembly was needed outside the pump, see Fig. 10b, therefore the measurements taken by the different pressure transducers were send to the data acquisition system. Further details on the test rig can be found in Haynes PhD [58].

In Fig. 10b, can also be seen a fourth pressure transducer located outside the pump, just before the pressure relief valve. This fourth transducer was used to measure the pressure ripple just outside the pump outlet.

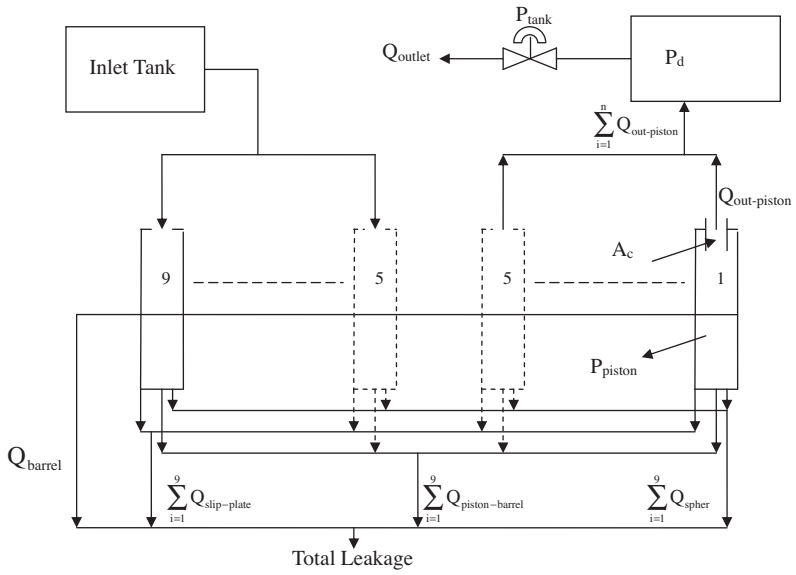

Fig. 9. A combine assembly of all pistons with nomenclature in axial piston pump.

The test rig used allowed to modify three parameters, turning speed, swash plate angle and output pressure. Test were performed for four different turning speeds, 200, 400, 700 and 1000 rpm, two swash plate angle tilts 10° and 20° and output pressures ranging from 1 to 10 MPa every 1 MPa. Hydraulic oil temperature was kept constant at 37 °C for all tests performed.

All information was captured using a PC based data logger, which allowed data to be directly captured onto a Microsoft windows based workstation.

11. Results

11.1. Experimental results

Fig. 11 presents the cylinder pressure ripple for 20° swash plate angle, 1000 rpm and for several output pressures, where it is noticed that the higher the output pressure will be, the higher is the pressure ripple inside the cylinder chamber. In fact, the pressure ripple in the cylinder chamber depends on the output pressure, the pump turning speed and swash plate angle. Pressure ripple is higher at high output pressures, high pump turning speeds and high swash plate angles. Fig. 12 shows the variation of pressure ripple for 10 MPa output pressure and 20° swash plate angle, as a function of different turning speeds, it is clearly seen that as turning speed decreases pressure ripple also decreases, at 1000 rpm the cylinder pressure ripple is of about 1 MPa, while at 400 rpm the peak to peak pressure ripple is less than 0.5 MPa. It is also noticed that the shape of pressure ripple changes with turning speed.

In Fig. 13 it is presented the cylinder pressure ripple variation as a function of swash plate angle, reducing the swash plate angle will bring a reduction of pressure ripple. It can be concluded that pressure ripple is primarily affected by output pressure being the effects of turning speed and swash plate angle, although important, less relevant than the output pressure ones.

Another interesting point which can be studied thanks to the experimentation undertaken is the relation between the pump output pressure, just before the pressure relief valve, see Fig. 10, and the pressure inside the cylinder chamber. For all the cases studied the output pressure was matching perfectly well the variations of cylinder pressure, output pressure was also under all conditions slightly lower than the pressure inside the cylinder chamber, such difference represents the pressure losses mostly inside the pump, since the pipe uniting the pump and the relief valve was very short. Pressure differential between the cylinder chamber and outside the pump, was found to be of about 0.25 MPa for 20° swash plate angle, 1000 rpm and 10 MPa output pressure, such pressure differential tends to slightly decrease with the decrease of the swash plate angle and slightly increases, about 0.05 MPa, with the decrease of output pressure, such increase it is understood when noticing that as the output pressure decreases, leakage decreases, therefore a slightly higher flow leaves the pump through the pump output port.

A decrease in pump turning speed brings a small decrease in pressure differential.

During experimentation, it was also noticed that cylinder pressure during the intake period, initially falls to a minimum and then increases a bit as the piston goes from the upper death centre to the lower death centre. The minimum pressure was found to be very near to 0 MPa, although just for a very short period of time. The pressure increase is more relevant for small turning speeds and high swash plate angles. Also for small turning speeds, it is seen that pressure does not remain constant when the piston goes from the lower death centre to the upper death centre, but it decreases as the piston moves towards the upper death centre, the decrease is higher for low turning speeds and higher pressures. This phenomena is very well understandable when considering that as turning speed decreases, the piston needs a longer time to go from LDC to UDC, giving more time to the fluid to escape across the clearances, barrel-plate and slipper port plate towards tank. This phenomenon can also be seen in Fig. 12, notice that the curves at 700 and 400 rpm decrease with angular position, hence with time.

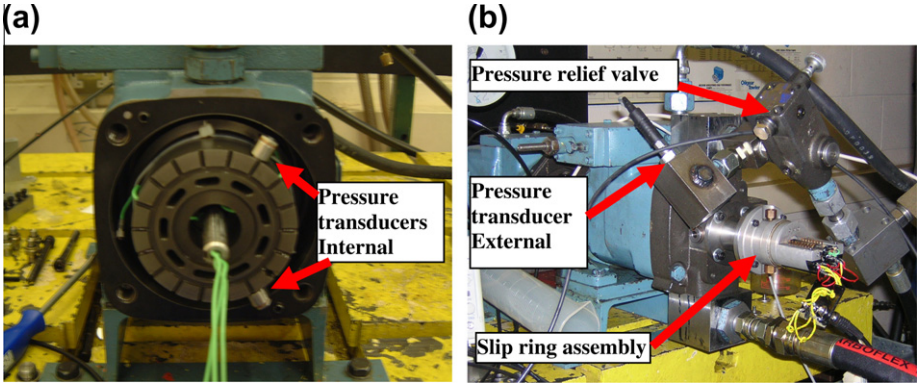

Fig. 10. Test rig used to measure directly the dynamic pressure inside a piston-cylinder chamber in an axial piston pump.

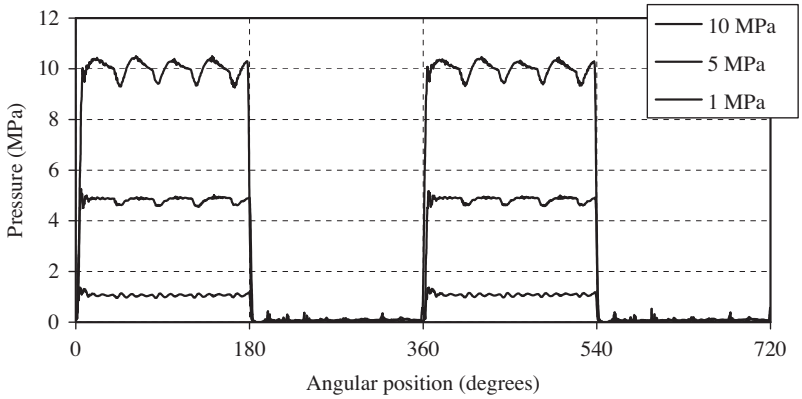

Fig. 11. Cylinder pressure ripple for 20° swash plate angle, 1000 rpm and several output pressures.

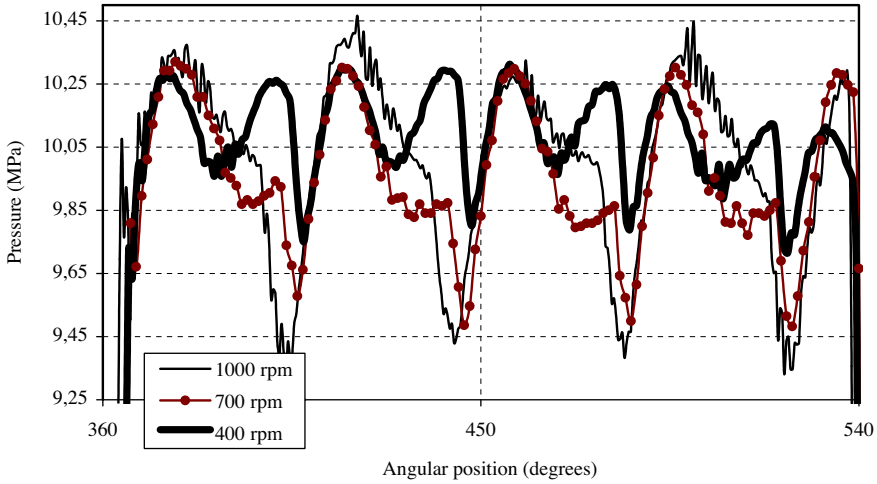

Fig. 12. Cylinder pressure ripple for 20° swash plate angle, 10 MPa and several pump turning speeds.

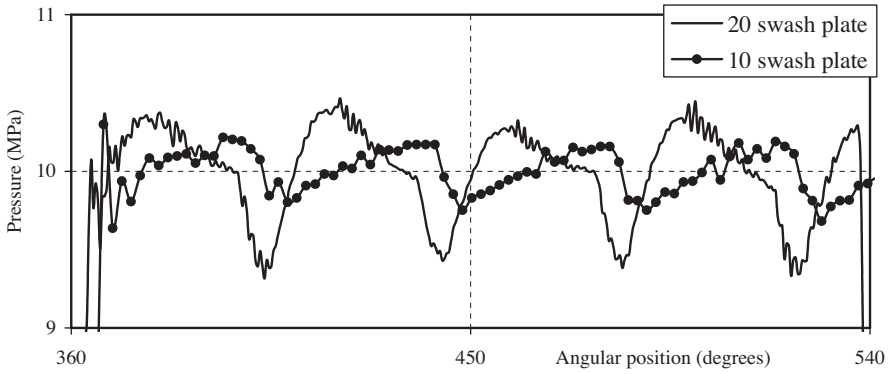

Fig. 13. Cylinder pressure ripple for an output pressure of 10 MPa, 1000 rpm and two swash plate angles.

11.2. Numerical results

Fig. 14 presents the dynamic pressure inside a piston chamber at 1000 rpm pump turning speed when the pressure relieve valve is set at 5 and 10 MPa outlet pressure. The barrel-port plate, slipper-swash plate, piston-cylinder and spherical bearing central clearances are assumed to be 5, 10, 5, 5 μm, respectively. The choice of the clearances, barrel-port plate

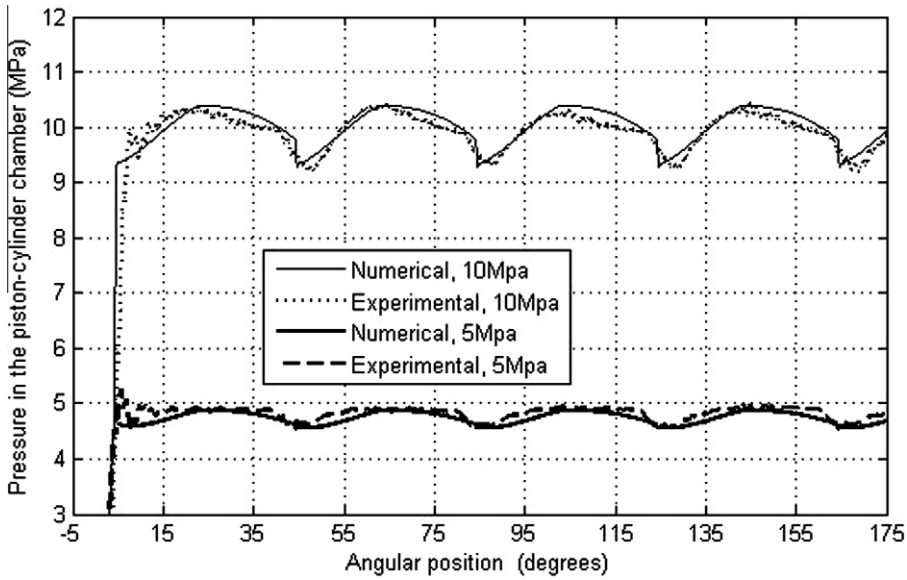

Fig. 14. Pressure inside piston at 5 and 10 MPa valve set pressure, 1000 rpm pump turning speed, comparison between numerical and experiments.

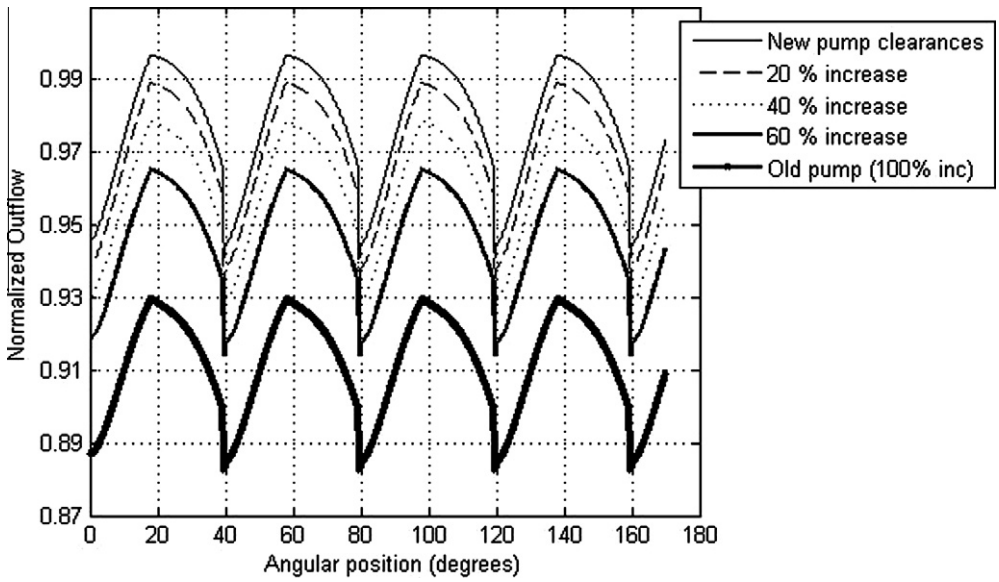

Fig. 15. Normalized temporal out flow from the pump as the pump clearances increases, set valve pressure 10 MPa, pump turning speed 1000 rpm. New pump clearances: slipper clearance 10 μm, barrel clearance 5 μm, spherical bearing clearance 5 μm and piston cylinder clearance 5 μm.

and slipper-swash plate, was based on literature [7,39,59], on the other hand the clearances for piston-cylinder and spherical bearing gap have been chosen based on manufacturers experience. Fig. 14 shows a very good agreement between numerical and experimental results.

Fig. 15 presents the normalized temporal outflow at 1000 rpm pump turning speed, 10 MPa outlet pressure, when being the new pump barrel, slipper, piston and spherical bearing clearances of 5, 10, 5, 5 μm respectively. In the same graph, it is presented the output flow ripple when the clearances increase in different percentages, simulating the pump erosion as it becomes old. It can be noticed, that regardless of the percentage increase in clearance, the shape of the temporal out flow ripple remains constant. Nevertheless the pump outflow decreases about 6% when the magnitude of the clearances doubles, which will result in a 6% decrease of volumetric efficiency.

Although not presented in the present paper, for the different clearances studied, the shape of the simulated pump output pressure ripple remains also constant.

Table 1 presents, for three different clearance configurations, the average leakage across all four piston pump gaps over one pump rotation. It can be noticed that when clearances in all gaps have the same magnitude, the leakage through barrel port plate is dominant, giving about 70% of the total piston pump leakage. It can also be seen that when all clearances double from 5 to 10 μm, the total pump leakage given as a percentage to the total output flow, increase from 0.6% to 4.6%. According to the literature [7,39,59], the slipper-port plate clearance is typically about 10 μm, and the barrel port plate clearance tends to fluctuate around 5 μm. The last two columns of Table 1 specify that under these conditions, the main leakage source for the present piston pump is the slipper-swash plate, producing around the 70% of the total leakage.

12. Conclusions

A set of new leakage equations developed by the authors in several different previous papers are validated via comparing them with Several CFD programs also previously developed by the authors.

A new piston pump model based on the new algebraic leakage equations is presented. The beauty of the model is its fast calculating speed and its good performance, since it is capable of simulating the pump output pressure ripple in great detail. The model has been validated using directly experimental measurements of the dynamic pressure inside a piston-cylinder chamber.

A novel, state of the art test rig, designed in Cardiff University and able to measure the dynamic pressure inside the cylinder in a piston pump has been presented. Dynamic pressure measurements inside the cylinder are being undertaken as a function of pump turning speed, outlet pressure and swash plate angle. The results clearly show how pressure ripple is being affected by such parameters; the output pressure being the parameter which more directly affects pressure ripple. The pressure ripple outside the pump follows with great detail the dynamic pressure ripple in a given cylinder, although it is about 0.25 MPa lower than the pressure inside the cylinder, such pressure differential is mostly due to the pressure losses in the pump output channels.

It is demonstrated that the main source of the leakage in piston pumps is weather the slipper-swash plate or the barrel-port plate, producing over 94% of the total leakage. Depending on the magnitude of the clearances slipper-swash plate and barrel-port plate, the main source of the leakage would be weather one gap or the other.

The pump output flow reduction is over 6% when all the clearances double. The output flow and pressure ripple shape is found to be independent of clearances magnitude.

Appendix 1

The one dimensional Reynolds equation of lubrication in Cartesian coordinates can be given as:

$$\frac{\partial}{\partial x}\left(\frac{h^3}{\mu}\frac{\partial p}{\partial x}\right)=0 \tag{A1}$$

and its integration yields

$$P=\frac{A\mu}{h^3}x+B. \tag{A2}$$

Eq. (A2) gives the pressure distribution along the "x" axis, and the constants A and B must be found using the boundary conditions.

The Couette–Poiseulle flow between two flat plates results in the following flow per unit depth:

$$\dot{\forall}=\frac{hu}{2}-\frac{\partial p}{\partial x}\frac{h^3}{12\mu}. \tag{A3}$$

Via substituting the first integration of Eq. (A1) in (A3) it is found that

$$\dot{\forall}=\frac{hu}{2}-\frac{A}{12}. \tag{A4}$$

Since Eqs. (A2) and (A4) are applicable to any pair of flat plates, then for each flat plate shown in Fig. 5 there exist a pair of equations as follows.

$$P_1=\frac{A\mu}{h_1^3}x+B, \tag{A5}$$

$$\dot{\forall}_1=\frac{h_1u}{2}-\frac{A}{12} \tag{A6}$$

range of applicability $0\leqslant x\leqslant l_1$ for the last flat plate:

$$P_{11}=\frac{U\mu}{h_{11}^3}x+V, \tag{A7}$$

$$\dot{\forall}_{11} = \frac{h_{11}u}{2} - \frac{U}{12}, \tag{A8}$$

$$\text{range of applicability } \left(\sum_{i=1}^{i=10} l_i\right) \leqslant x \leqslant \left(\sum_{i=1}^{i=11} l_i\right). \tag{A9}$$

The constants $A \ldots V$ have to be found using boundary conditions in both piston ends and in each pair of connected surfaces.

In this study the analysis results in 22 equations with 22 unknown constants.

In any connection of two surfaces:

$$x = \sum_{j=1}^{j=i} l_j; \quad P_i = P_{i+1}; \quad \dot{V}_i = \dot{V}_{i+1}; \quad 1 \leqslant i \leqslant 10. \tag{A10}$$

If it is assumed that:

$$\begin{aligned} &l_2 = l_4 = l_6 = l_8 = l_{10}; \quad l_3 = l_5 = l_7 = l_9; \\ &h_1 = h_3 = h_5 = h_7 = h_9 = h_{11}; \quad h_2 = h_4 = h_6 = h_8 = h_{10}. \end{aligned} \tag{A11}$$

The value of the constants will be:

$$A = \frac{P_{\tan k} - P_{\text{piston}} - C_{A2}}{\frac{\mu}{h_{11}^3}\sum_{i=1}^{i=11} l_i + C_{A1}}. \tag{A12}$$

In the case under study:

$$A = E = I = M = Q = U; \quad B = P_{\text{piston}}; \tag{A13}$$

$$C_{A1} = \mu\left[\frac{1}{h_2^3} - \frac{1}{h_1^3}\right](l_2 + l_4 + l_6 + l_8 + l_{10}), \tag{A14}$$

$$C_{A2} = 6u\mu\left[\frac{h_{10} - h_1}{h_{10}^3}(l_2 + l_4 + l_6 + l_8 + l_{10})\right]. \tag{A15}$$

According to the previous specifications:

$$C = K = G = O = S = 6u(h_2 - h_1) + A, \tag{A16}$$

$$D = A\mu\left[\frac{1}{h_1^3} - \frac{1}{h_2^3}\right] * (l_1) + 6u\mu\left[\frac{h_2 - h_1}{h_2^3}\right] * (-l_1) + B; \tag{A17}$$

$$F = A\mu\left[\frac{1}{h_2^3} - \frac{1}{h_1^3}\right] * (l_2) + 6u\mu\left[\frac{h_2 - h_1}{h_2^3}\right] * (l_2) + B; \tag{A18}$$

$$H = A\mu\left[\frac{1}{h_1^3} - \frac{1}{h_2^3}\right] * (l_1 + l_3) + 6u\mu\left[\frac{h_2 - h_1}{h_2^3}\right] * (-(l_1 + l_3)) + B; \tag{A19}$$

$$J = A\mu\left[\frac{1}{h_2^3} - \frac{1}{h_1^3}\right] * (l_2 + l_4) + 6u\mu\left[\frac{h_2 - h_1}{h_2^3}\right] * (l_2 + l_4) + B, \tag{A20}$$

$$L = A\mu\left[\frac{1}{h_1^3} - \frac{1}{h_2^3}\right] * (l_1 + l_3 + l_5) + 6u\mu\left[\frac{h_2 - h_1}{h_2^3}\right] * (-(l_1 + l_3 + l_5)) + B; \tag{A21}$$

$$N = A\mu\left[\frac{1}{h_2^3} - \frac{1}{h_1^3}\right] * (l_2 + l_4 + l_6) + 6u\mu\left[\frac{h_2 - h_1}{h_2^3}\right] * (l_2 + l_4 + l_6) + B; \tag{A22}$$

$$P = A\mu\left[\frac{1}{h_1^3} - \frac{1}{h_2^3}\right] * (l_1 + l_3 + l_5 + l_7) + 6u\mu\left[\frac{h_2 - h_1}{h_2^3}\right] * (-(l_1 + l_3 + l_5 + l_7)) + B, \tag{A23}$$

$$R = A\mu\left[\frac{1}{h_2^3}-\frac{1}{h_1^3}\right]*(l_2+l_4+l_6+l_8)+6u\mu\left[\frac{h_2-h_1}{h_2^3}\right]*(l_2+l_4+l_6+l_8)+B; \tag{A24}$$

$$T = A\mu\left[\frac{1}{h_1^3}-\frac{1}{h_2^3}\right]*(l_1+l_3+l_5+l_7+l_9)+6u\mu\left[\frac{h_2-h_1}{h_2^3}\right]*(-(l_1+l_3+l_5+l_7+l_9))+B, \tag{A25}$$

$$V = A\mu\left[\frac{1}{h_2^3}-\frac{1}{h_1^3}\right]*(l_2+l_4+l_6+l_8+l_{10})+6u\mu\left[\frac{h_2-h_1}{h_2^3}\right]*(l_2+l_4+l_6+l_8+l_{10})+B. \tag{A26}$$

With these set of equations, it is now possible to find the pressure distribution along the piston length, for a piston with five slots. In fact, the equations allow to investigate the pressure increase on each slot when different piston velocities are considered, see Bergada and Watton [52].

It is traditionally assumed that the leakage due to the gap piston cylinder is constant, and has a linear relationship with the pressure differential of the piston ends. In fact, if the previous results are considered it can clearly be seen that the leakage flow depends on the relative movement of the piston which could well be significant in practice. Since the piston velocity is sinusoidal the leakage will also be affected. The piston velocity can be given as:

$$u = -R_p\tan\varepsilon\sin(\omega t)\omega. \tag{A27}$$

Substituting this equation into each leakage flow for real piston movement, results in the flow equation (A28)

$$q_{\text{piston-barrel}} = \pi d\left[\frac{h_1 R_p\tan\varepsilon(-\sin(\omega t))\omega}{2}\right] - \frac{\pi d}{12}\left[\frac{P_{\text{tank}}-P_{\text{piston}}-6R_p\tan\varepsilon(-\sin(\omega t))\omega\mu\left[\frac{h_{10}-h_1}{h_{10}^3}\right](l_2+l_4+l_6+l_8+l_{10})}{\frac{\mu}{h_{11}^3}(l_1+l_2+l_3+\ldots+l_{11})+\mu\left[(\frac{1}{h_2^3}-\frac{1}{h_1^3})(l_2+l_4+l_6+l_8+l_{10})\right]}\right]. \tag{A28}$$

Eq. (A28) assumes that the piston is always inside the barrel, but in reality this is not true since the piston length inside the barrel changes temporally, once the real piston length inside the barrel is taken into account equation from (A27), the resulting piston-barrel dynamic leakage will be given in Eq. (A29).

$$q_{\text{piston-barrel}} = \pi d\left[\frac{h_1 R_p\tan\varepsilon(-\sin(\omega t))\omega}{2}\right] - \frac{\pi d}{12}\left[\frac{P_{\text{tank}}-P_{\text{piston}}-6R_p\tan\varepsilon(-\sin(\omega t))\omega\mu\left[\frac{h_{10}-h_1}{h_{10}^3}\right](l_2+l_4+l_6+l_8+l_{10})}{\frac{\mu}{h_{11}^3}(l_1+l_2+l_3+\ldots+l_{11}-\frac{0.0195}{2}-R_p\tan\varepsilon\cos(\omega t))+\mu\left[(\frac{1}{h_2^3}-\frac{1}{h_1^3})(l_2+l_4+l_6+l_8+l_{10})\right]}\right]. \tag{A29}$$

Equation which will give the temporal leakage piston barrel, for any clearance, pressure distribution, and pump turning speed. At time $t = 0$, it has to be understood that the piston is at its bottom death centre.

References

[1] K. Foster, D.M. Hannan, Fundamental fluidborne and airborne noise generation of axial piston pumps, in: Seminar on Quiet Oil Hydraulic Systems, Paper C257/77, Institution of Mechanical Engineers, London, England, 1977.
[2] N.D. Manring, The discharge flow ripple of an axial-piston swash-plate type hydrostatic pump, J. Dyn. Syst. Measure. Control, ASME 122 (2000) 263–268.
[3] N.D. Manring, F.A. Damtew, The control torque on the swash plate of an axial piston pump utilizing piston-bore springs, J. Dyn. Syst. Measure. Control, ASME 123 (2001) 471–478.
[4] N.D. Manring, Y. Zhang, The improved volumetric efficiency of an axial-piston pump utilizing a trapped-volume design, J. Dyn. Syst. Measure. Control, ASME 123 (2001) 479–487.
[5] M. Ivantysynova, C. Huang, Investigation of the flow in displacement machines considering elastohydrodynamic effect, in: Proceedings of the Fifth JFPS International Symposium on Fluid Power, Nara 2002, Japan, November 13, vol. 1, pp. 219–229.
[6] M. Ivantysynova, J. Grabbel, J.C. Ossyra, Prediction of a swash plate moment using the simulation tool CASPAR, in: ASME International Mechanical Engineering Congress and Exposition, 2002, New Orleans, Louisiana USA, November 17–22, IMECE2002-39322, pp. 1–9.
[7] U. Wieczorek, M. Ivantysynova, Computer aided optimization of bearing and sealing gaps in hydrostatic machines – the simulation tool CASPAR, Int. J. Fluid Power 3 (1) (2002) 7–20.
[8] M. Ivantysynova, A new approach to the design of sealing and bearing gaps of displacement machines, in: Fluid Power Fourth JHPS International Symposium, 1999, pp. 45–50.
[9] M. Ivantysynova, R. Lasaar, An investigation into micro- and macrogeometric design of piston/cylinder assembly of swash plate machines, Int. J. Fluid Power 5 (1) (2004) 23–36.
[10] J. Ma, B. Fang, B. Xu, H. Yang, Optimization of cross angle based on the pumping dynamics model, J. Zhejiang Univ. Sci. A 11 (3) (2010) 181–190.
[11] B.O. Helgestad, K. Foster, F.K. Bannister, Pressure transients in an axial piston hydraulic pump, in: Proceedings of the Institution of Mechanical Engineers, vol. 188, No. 17/74, 1974, pp. 189–199.
[12] M.J. Martin, B. Taylor, Optimised port plate timing for an axial piston pump, in: Fifth International Fluid Power Symposium, Cranfield, England, September 13–15, 1978, pp. B5-51–B5-66.
[13] K.A. Edge, J. Darling, The pumping dynamics of swash plate piston pumps, J. Dyn. Syst. Measure. Control, ASME 111 (1989) 307–312.

[14] G. Jacazio, F. Vatta, The block-lift in axial piston hydraulic motors, in: The ASME/ASCE Bioengineering, Fluids Engineering and Applied Mechanics Conference, Boulder, Colorado, USA, June 22–24, 1981 pp. 1–7.
[15] A. Yamaguchi, Formation of a fluid film between a valve plate and a cylinder block of piston pumps and motors (2nd report, a valve plate with hydrostatic pads), Int. J. Jpn. Soc. Mech. Eng. 30 (259) (1987) 87–92.
[16] A. Yamaguchi, Bearing/seal characteristics of the film between a valve plate and a cylinder block of axial piston pumps: effects of fluid types and theoretical discussion, J. Fluid Control 20 (4) (1990) 7–29.
[17] K. Matsumoto, M. Ikeya, Friction and leakage characteristics between the valve plate and cylinder for starting and low speed conditions in a swashplate type axial piston motor, Trans. Jpn. Soc. Mech. Eng. C 57 (538) (1991) 2023–2028.
[18] K. Matsumoto, M. Ikeya, Leakage characteristics between the valve plate and cylinder for low speed conditions in a swashplate-type axial piston motor, Trans. Jpn. Soc. Mech. Eng. C 57 (1991) 3008–3012.
[19] S. Kobayashi, K. Matsumoto, Lubrication between the valve plate and cylinder block for low speed conditions in a swashplate-type axial piston motor, Trans. Jpn. Soc. Mech. Eng. C 59 (561) (1993) 182–187.
[20] G. Weidong, W. Zhanlin, Analysis for the real flow rate of a swash plate axial piston pump, J. Beijing Univ. Aeronaut. Astronaut. 22 (2) (1996) 223–227.
[21] A. Yamaguchi, Tribology of hydraulic pumps, ASTM Spec. Tech. Publ. (1310) (1997) 49–61.
[22] A. Yamaguchi, H. Sekine, S. Shimizu, S. Ishida, Bearing/seal characteristics of the oil film between a valve plate and a cylinderblock of axial pumps, JHPS 18-7 (1987) 543–550.
[23] N.D. Manring, Tipping the cylinder block of an axial-piston swash-plate type hydrostatic machine, ASME J. Dyn. Syst. Measure. Control 122 (2000) 216–221.
[24] N.D. Manring, Valve-plate design for an axial piston pump operating at low displacements, ASME J. Mech. Eng. 125 (2003) 200–205.
[25] J.M. Bergada, J. Watton, S. Kumar, Pressure, flow, force and torque between the barrel and port plate in an axial piston pump, ASME J. Dyn. Syst. Measure. Control. 130 (2008) 011011-1–011011-16.
[26] M.J. Fisher, A theoretical determination of some characteristics of a tilted hydrostatic slipper bearing, B.H.R.A. Rep. RR, 1962, p. 728.
[27] O. Böinghoff, Untersuchen zum Reibungsverhalten der Gleitschuhe in Schrägscheiben-Axialkolbenmascinen, VDI-Forschungsheft, vol. 584, VDI-Verlag, 1977. pp. 1–46.
[28] C.J. Hooke, Y.P. Kakoullis, The lubrication of slippers on axial piston pumps, in: Fifth International Fluid Power Symposium, B2-(13-26), Durham, England, September 1978.
[29] C.J. Hooke, Y.P. Kakoullis, The effects of centrifugal load and ball friction on the lubrication of slippers in axial piston pumps, in: Sixth International Fluid Power Symposium, Cambridge, England, 1981, pp. 179–191.
[30] N. Iboshi, A. Yamaguchi, Characteristics of a slipper bearing for swash plate type axial piston pumps and motors, theoretical analysis, Bull. JSME 25 (210) (1982) 1921–1930.
[31] N. Iboshi, A. Yamaguchi, Characteristics of a slipper bearing for swash plate type axial piston pumps and motors, experiment, Bull. JSME 26 (219) (1983) 1583–1589.
[32] C.J. Hooke, Y.P. Kakoullis, The effects of non flatness on the performance of slippers in axial piston pumps, Proc. Inst. Mech. Eng. C 197 (1983) 239–247.
[33] C.J. Hooke, K.Y. Li, The lubrication of overclamped slippers in axial piston pumps centrally loaded behaviour, Proc. Inst. Mech. Eng. 202 (C4) (1988) 287–293.
[34] C.J. Hooke, K.Y. Li, The lubrication of slippers in axial piston pumps and motors. The effect of tilting couples, Proc. Inst. Mech. Eng. C 203 (1989) 343–350.
[35] K. Takahashi, S. Ishizawa, Viscous flow between parallel disks with time varying gap width and central fluid source, in: JHPS International Symposium on Fluid Power, Tokyo, March 1989, pp. 407–414.
[36] K.Y. Li, C.J. Hooke, A note on the lubrication of composite slippers in water based axial piston pumps and motors, Wear 147 (1991) 431–437.
[37] E. Koc, C.J. Hooke, K.Y. Li, Slipper balance in axial piston pumps and motors, Trans. ASME, J. Tribol. 114 (1992) 766–772.
[38] S. Kobayashi, M. Hirose, J. Hatsue, M.. Ikeya, Friction characteristics of a ball joint in the swashplate type axial piston motor, in: Proceedings of the Eighth International Symposium on Fluid Power, J2 Birmingham, England, 1988, pp. 565–592.
[39] R.M. Harris, K.A. Edge, D.G. Tilley, Predicting the behaviour of slipper pads in swashplate-type axial piston pumps, in: ASME Winter Annual Meeting, New Orleans, Louisiana, November 28–December 3, 1993, pp. 1–9.
[40] E. Koc, C.J. Hooke, Investigation into the effects of orifice size, offset and oveclamp ratio on the lubrication of slipper bearings, Tribol. Int. 29 (4) (1996) 299–305.
[41] E. Koc, C.J. Hooke, Considerations in the design of partially hydrostatic slipper bearings, Tribol. Int. 30 (11) (1997) 815–823.
[42] T. Tsuta, T. Iwamoto, T. Umeda, Combined dynamic response analysis of a piston-slipper system and lubricants in hydraulic piston pump, Emerg. Technol. Fluids Struct. Fluid/Struct. Interact. ASME 396 (1999) 187–194.
[43] U. Wieczoreck, M. Ivantysynova, CASPAR – a computer aided design tool for axial piston machines, in: Proceedings of the Power Transmission Motion and Control International Workshop, PTMC2000, Bath, UK, 2000, pp. 113–126.
[44] Y.P. Kakoulis, Slipper Lubrication in Axial Piston Pumps, M.Sc. Thesis, University of Birmingham, 1977.
[45] J.M. Bergada, J.M. Haynes, J. Watton, Leakage and groove pressure of an axial piston pump slipper with multiple lands, Tribol. Trans. 51 (2008) 469–482.
[46] J.M. Bergada, J. Watton, J.M. Haynes, D.L. Davies, The hydrostatic/hydrodynamic behaviour of an axial piston pump slipper with multiple lands, Meccanica 45 (4) (2010) 585–602.
[47] S. Kumar, CFD Analysis of an Axial Piston Pump, PhD Thesis from UPC, Spain, 2010.
[48] S. Kumar, J.M. Bergada, J. Watton, Axial piston pump grooved slipper analysis by CFD simulation of three-dimensional NVS equation in cylindrical coordinates, Comput. Fluids 38 (2009) 648–663.
[49] M. Milani, Design hydraulic locking balancing grooves, Proc. Inst. Mech. Eng. 215 (Part I) (2001) 453–465.
[50] M. Borghi, G. Cantore, M. Milani, P. Paoluzzi, Numerical analysis of the lateral forces acting on spools of hydraulic components, FPST5, Fluid Power Systems and Technology, ASME, 1998.
[51] M. Borghi, Hydraulic locking-in spool-type valves: tapered clearances analysis, Proc. Inst. Mech. Eng. 215 (Part I) (2001) 157–168.
[52] J.M. Bergada, J. Watton, A new approach towards the understanding of the flow in small clearances applicable to hydraulic pump pistons with pressure balancing grooves, in: Seventh International Symposium on Fluid Control, Measurement and Visualization, Flucome 2003, Sorrento, Italy, August 25–28, pp. 1–8.
[53] K. Abe, M. Imai, E. Kometani, The performance of ball-piston multi-stroke type low speed high torque motor (report N 1, experimental study on performance of spherical surface of piston), Bull. JSME 22 (167) (1979) 700–706.
[54] K. Abe, K. Ono, The performance of ball-piston multi-stroke type low speed high torque motor (2nd report practical analysis on multi-stroque type cam profile), Trans. Jpn. Soc. Mech. Eng. B 395 (1979) 974–981.
[55] S. Kobayashi, M. Ikeya, Elastohydrostatic lubrication of piston balls and hydrostatic slipper bearings in swashplate type axial piston motors, in: Tenth International Conference on Fluid Power – the future for Hydraulics, Brugge, Belgium, 5–7 April 1993, pp. 311–322.
[56] D. Meyer, Reynolds equation for spherical bearings, J. Tribol. ASME 125 (2003) 203–206.
[57] J. Watton, Fundamentals of Fluid Power Control, Cambridge University Press, 2009.
[58] J.M. Haynes, Axial Piston Pump Leakage Modeling and Measurement, PhD Thesis from Cardiff University, UK, 2008.
[59] J.M. Bergada, D.Ll. Davies, S. Kumar, J. Watton, The effect of oil pressure and temperature on barrel film thickness and barrel dynamics of an axial piston pump, Meccanica (2011), doi:10.1007/s11012-011-9472-7.